# Third Semiannual Report

# A STUDY OF THE ELECTROTRANSPORT IN THIN FILMS

NASA Research Grant
NGR 10-005-080

Submitted to:

NATIONAL AERONAUTICS AND SPACE ADMINISTRATION

Submitted by:
DEPARTMENT OF METALLURGICAL AND MATERIALS ENGINEERING
UNIVERISTY OF FLORIDA
GAINESVILLE, FLORIDA 32601

R. E. Hummel, Chief Investigator

For the period

May 1, 1969 - October 31, 1969

# 1. Introduction

The ultimate goal of this research project is to understand the mechanisms which are involved in thin film electrotransport. After careful consideration of the various methods to attack this problem three general ideas were selected. They are:

1. High precision electrical resistance measurements of several small portions of a thin film strip during electrotransport. This method was selected because it gives fairly fast quantitative results on the kinetics of the processes involved. This research tool is now in a stage where a large number of experimental tests can be performed with various samples and in different environments.
2. Radioactive tracer method. This method will be used to supplement the resistance data and to get additional insight into the mechanisms of electrotransport. Despite the fact that our department has substantial experience in studies using radioactive tracer methods, it was found that further development of these methods must be completed before experiments on a larger scale can be started. The preliminary results have been very promising.

3. The scanning electron microscope which was recently purchased by this department will be employed to further supplement our findings.

In the following sections, the principal results of our investigations and our plans for further studies will be described.

## 2. Research Objectives

To obtain some insight into the failure mechanism of thin films the simplest method immediately at hand, is to examine the dependence of lifetime on various parameters. Several investigators determined the dependence of mean time to failure on temperature, current density, grain size and condition of the surface. From these experiments it is possible to calculate an activation energy, which gives an indication of the type of diffusion process mainly operative in the film. This method may be well suited to give a first survey, but it cannot replace a more thorough investigation. The thin films often fail at irregularities, which means that the lifetime data have more or less a statistical character. In addition, the relationship between mass transport rate and lifetime is not necessarily straightforward and some assumptions have to be made. It is therefore felt that there is a need for more accurate methods to determine transport rates in thin films. It is hoped that the following information can be obtained:

1. By measuring the mass transport at different temperatures the activation energy of the electrotransport process can be determined more accurately than with the lifetime method. As mentioned above, this parameter is of great interest, because it indicates whether surface diffusion, grain boundary diffusion or volume diffusion is dominant.

2. The dependency of electrotransport rate on current density. There is some discrepancy between the theories of different authors. Huntington and several other investigators predict a linear relationship between electrotransport rate and current density, whereas Black claims a dependency on $(\text{current density})^2$.
3. Determination of effective valence.
4. It will be interesting to learn how the migration rate changes when some thin film parameters are varied, such as thickness, structure, grain size and surface condition. This should give an indication as to what steps should be taken to improve the lifetime of integrated circuits.

## 3. Investigations of Electrotransport by Measuring the Electrical Resistance

Our primary research effort in using resistance techniques has been directed toward the accumulation of data and the refinement of our sample design. More than one hundred tests have been performed, using various sample designs in different environmental conditions, in order to pinpoint the principal phenomena that effect the mechanisms and kinetics of electrotransport in thin films. The method of using resistivity measurements has proven to be very valuable in monitoring the formation of voids. Although this method seems to have certain limitations, our studies have shown that with appropriate sample and experimental design, this technique can be useful in understanding the basic mechanisms of electrotransport in thin films.

### 3.1. Experimental Procedure

In the course of our investigations, various sample designs have been used and identical experiments, with respect to current density and environment, have been performed with these specimens. By proper interpretation, all these experiments led to the same basic result. Below, the designs of the various specimens are described.

Pure aluminum samples were prepared, using the mask shown in Fig. 1, and subjected to D. C. current densities of about $5 \times 10^5$ amps per square centimeter in an air environment. Resistance measurements were made periodically and plotted

versus time. One problem encountered with this particular sample design is that it is impossible to monitor possible changes in resistance to the left of area number I. Therefore, the design was modified to that shown in Fig. 2. Specimens of type 1 and 2 possess two wider parts (A) at the ends of the stripe. This design could cause curved potential lines in the specimen just at the critical point B where the voids are usually first observed. In order to overcome this, composite samples were made using silver for the electrodes and aluminum for the gage section. Silver proved to be better than other materials, such as Cr or Ni due to its low electrical resistivity and its low diffusion coefficient. Normally a thickness of about 8,000 angstroms of silver was deposited first, then an aluminum film of an approximate thickness of 1,500-2,000 Å was vapor deposited, overlapping the silver by about 1 millimeter at each end. The overlap takes place in the area directly below the second and fifth potential leads (Fig. 3). Due to the much thicker silver film and the higher melting point of silver compared to aluminum, the electrotransport in the silver layer is so small that it can be neglected.

In a further modification, the overlap areas were shifted towards the center so that the aluminum portion was totally confined between potential leads number 2 and 5 (Fig. 4). This design places the critical zone B, in which void formation is usually detected in a larger amount, completely into area II, whereas in the sample type of Fig. 3 the voids formed

in zone B are altering the resistance of area II as well as the one of area I.

So far most of the experiments were performed in a styrofoam container with a wall thickness of about 10 cm. in order to assure constant temperatures after an initial warm-up period. The temperature distribution along some typical samples were measured with a small thermocouple.

The preparation of the masks by chemical milling and the samples by high vacuum evaporation was described in the "Second Semiannual Report."

## 3.2. Results

In this section, some typical curves are presented which were obtained with resistance measurements. In Figs. 5, 6 and 7 the relative resistance change of the five areas marked in Figs. 1 through 4 are plotted versus time. In addition, the average specimen temperature measured near the middle of the sample (Point C in Fig. 8) is shown. The end-point of these curves mark always the failure of the sample due to opening of the circuit. The following items can be seen:

1. All curves have in common that after the specimen temperature has reached a fairly constant value, the resistance change in areas III, IV and V is extremely small.
2. All curves show that the resistance of that area which, looking in the direction of current flow, first has a smaller cross-sectional area (i.e., area

II in Fig. 2 and 4 and area I in Fig. 1) increases substantially with time. This is seen in Figs. 5 through 7.

3. The resistance of area I in Fig. 6 decreases with time.
4. Near the end of the experiment, i.e. shortly before failure, the temperature is increasing.
5. In Fig. 5, Curve No. I shows two pronounced steps of resistance increase, namely a fairly shallow one until about 80 hours and a steep one from 80 hours until failure. The samples whose resistance curves are plotted in Figs. 6 and 7 and which were subjected to about 8% higher current densities show only the steep increase in resistance.
6. In the sample which is represented by Fig. 5, the time until failure is about 10 times as large as for the specimens of Figs. 6 and 7 which were subjected to higher current densities.

In Fig. 8, the temperature distribution of a sample of the type of Fig. 4 is presented. A temperature gradient across the length of the sample as well as across the width can be noted. The latter is due to the potential leads which act as heat sinks.

In order to find out whether part of the resistance changes, shown in Figs. 5 through 7, are due to annealing, several samples were subjected to alternating current under otherwise identical conditions. No resistance change was

observed in this experiment, which shows that the observed effects are merely due to electrotransport.

Figure 9 shows schematically a portion of a pure Al sample after it was run to failure. It is interesting to note that void formation can be seen in two general areas:

1. In large amounts in area B, as expected.
2. Smaller voids on the potential leads (area D). The latter effect may be due to the heat drain which is caused by the potential leads.

All the films of the experiments mentioned above were deposited on glass substrates. In addition, similar experiments were undertaken with silicon wafers as a substrate. Basically, the same features were observed with one difference: The lifetime of the films on silicon wafers was at least 10 times larger than on glass substrates.

# 4. Radioactive Tracer Method

## 4.1. Sample Preparation

At present two different methods are used to activate a small area in the middle of a gold strip. This activation is done to monitor the amount of mass transport due to electromigration.

The first method uses thin gold films which were deposited in high vacuum on a silicon wafer (Fig. 10). Then an area 1 x 2 mm was subjected to thermal neutrons. Before placing the wafer into the thermal column of a nuclear reactor, the sample was covered on both sides with Cd-sheet 0.8 mm in thickness. A small hole in one of the Cd-sheets (1 x 2 mm) is so positioned that it lies over the middle of the gold strip. The Cd-sheet acts as a shield against thermal neutrons. To keep the amount of fast neutrons as low as possible, the whole assembly was placed inside a paraffin block, which acted as moderator. Irradiation time was between 6 and 8 hours at a thermal neutron flux of approximately $10^6$ neutrons/$cm^2$ sec. The second method which is currently in use requires two evaporations. First, the middle part of the gold film is deposited in high vacuum on the silicon wafer. The sample is then put in the nuclear reactor, but this time without any Cd-shielding. After approximately one day the activity of the silicon has decayed sufficiently, and the outer parts of the sample can be deposited.

## 4.2. Monitoring of the Radioactive Region

The position of the radioactive region is monitored by mounting the specimen on a precision mechanical stage of an optical measuring microscope and traversing it horizontally under a scintillation crystal-photomultiplier assembly.

In order to make the crystal as insensitive as possible to $\gamma$-radiation, its dimensions are kept very small (5 x 3 x 2 mm). A shielding plate for $\beta$-rays is made of stainless steel (4 mm thick) with a small adjustable slit (width variable between 100 and 300$\mu$) and interposed between the scintillator and the specimen. The sample is traversed beneath the slit in small increments by means of the mechanical stage mentioned above, and the activity at each position is measured. This measurement is performed before and after applying D. C. current to the film. The difference between the two measurements indicates the shift of the active region due to electrotransport.

## 4.3. Results

Figure 11 shows a typical curve which was obtained using the first method mentioned above. In this plot the number of counts in an interval of 30 minutes is plotted versus various positions of the counter across the sample. The second method is still being developed at this time. Results from it will be reported in the next semiannual report.

## 5. Discussion and Future Plans

It is too early at this stage to give a comprehensive interpretation of the results. Some typical phenomenological features of electrotransport which were observed by other investigators were confirmed.

Due to the loss of material, the resistance increases. This occurs at the "cathode" or more definitely, in the area which, looking in the direction of current flow, first has a smaller cross-sectional area. The material would be expected to be deposited at the opposite end of the strip and it is expected that the resistance decreases in this area (for example, in area IV or V). This was, however, never observed. Two possibilities for interpretation of this surprising result are currently under investigation:

1. The material may be deposited on the "colder" potential leads. To decrease this possible effect the width of the potential leads has been reduced by 75% of the original width. Investigations with this modified sample design are in progress.
2. The transported material is deposited in the form of whiskers and therefore does not contribute to the conduction. Scanning electron microscopy studies are in progress to look into this possibility.

The research program for the next year includes the variation of sample environment, substrate, temperature gradient

and film structure. Details on this are included in last year's Renewal Proposal.

In order to obtain reproducible film thicknesses a rate meter is needed for inclusion into our high vacuum evaporation unit. It is further planned to install a substrate heater in this piece of equipment to be able to vary the film structure. The radioactive tracer method will be applied as outlined in section 4, in addition to the resistance method described in section 3.

## Figure Captions

Figures 1-4 Shapes of specimens used for resistance measurements

Figure 5 Relative resistance and temperature of an Al specimen of type 1 (Fig. 1) versus time. Environment: air. Current density = $4.0 \times 10^5$ A/cm$^2$; sample thickness = 1,950 Å; substrate = glass. The numbers on the curves refer to the area numbers (see Fig. 1).

Figure 6 Relative resistance and temperature of an Al specimen of type 2 (Fig. 2) versus time. Environment = air; current density = $4.4 \times 10^5$ A/cm$^2$; sample thickness = 1,240 Å; substrate = glass.

Figure 7 Relative resistance and temperature of an Al sample of type 4 (Fig. 4) versus time. Environment = air; current density = $4.3 \times 10^5$ A/cm$^2$; sample thickness = 2,145 Å; substrate = glass.

Figure 8 Temperature distribution across a sample of type 4 (Fig. 4).

Figure 9 Sketch of the sample of Fig. 6 after failure. The dots are voids.

Figure 10 Shape of a gold sample as used for radioactive tracer experiments. The shaded area (a) is activated.

Figure 11 Typical curve obtained by scanning a scintillation counter across an activated area of a sample of type 10 (Fig. 10).

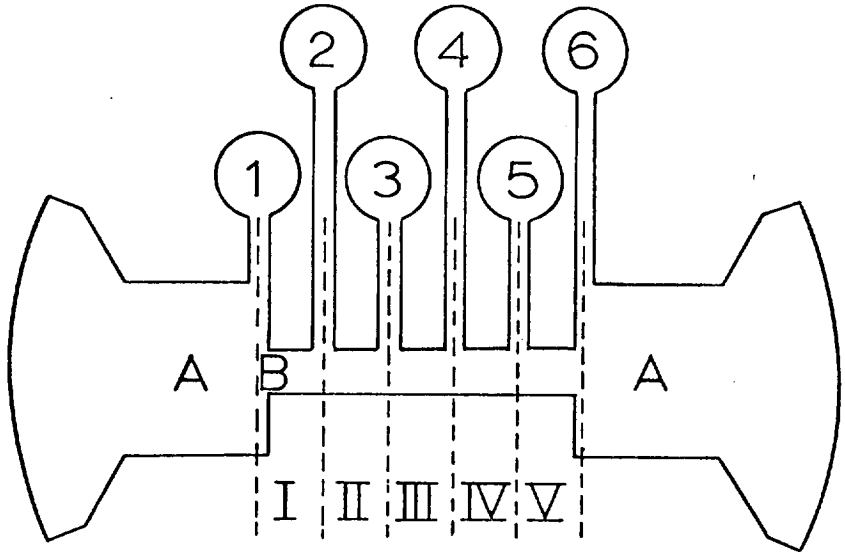


FIG. 1

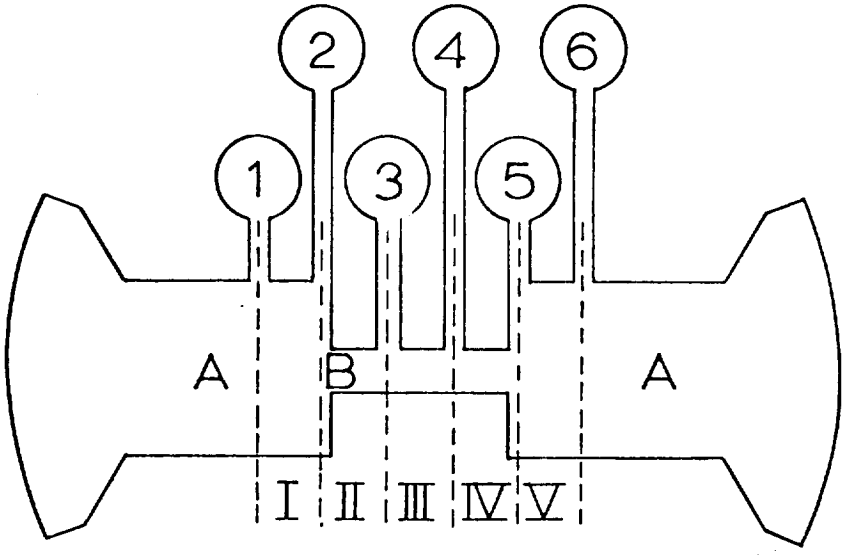


FIG. 2

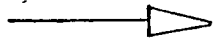

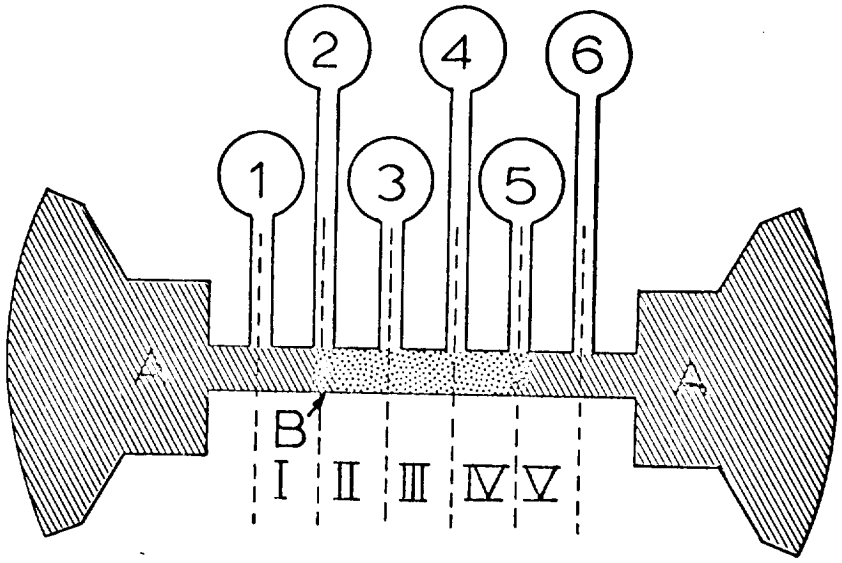


FIG. 3

Ag

Al

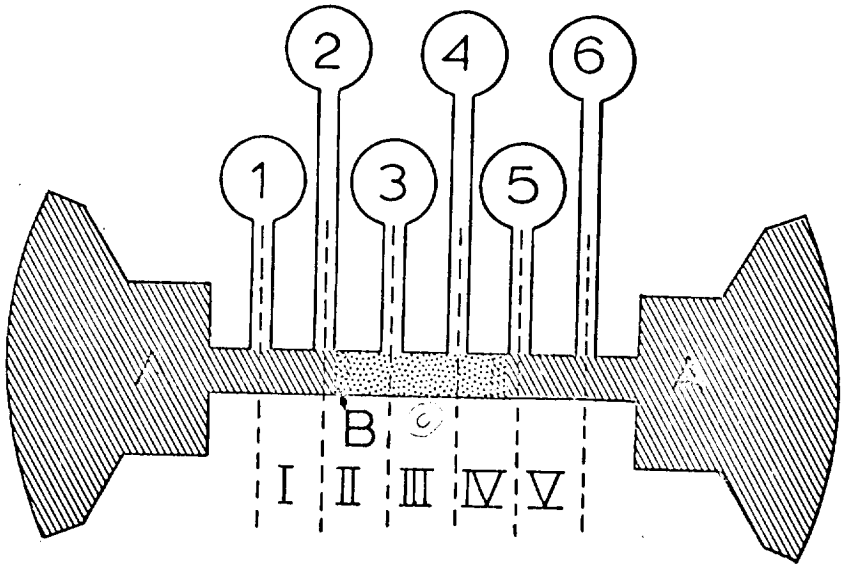


FIG. 4

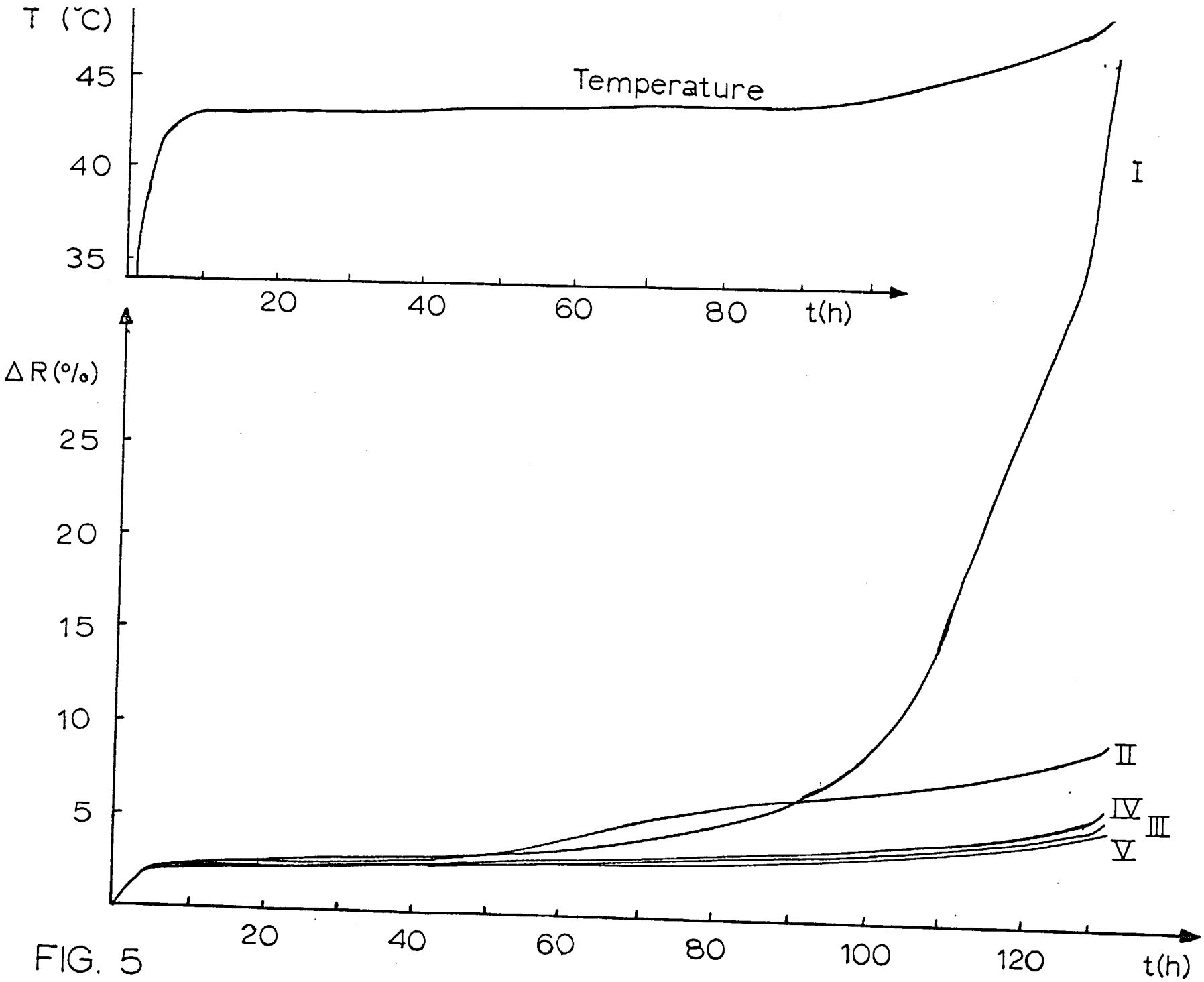
T (°C)
45
40
35
Temperature
20
40
60
80
t(h)
I
ΔR(%)
25
20
15
10
5
II
IV
III
V
20
40
60
80
100
120
t(h)

FIG. 5

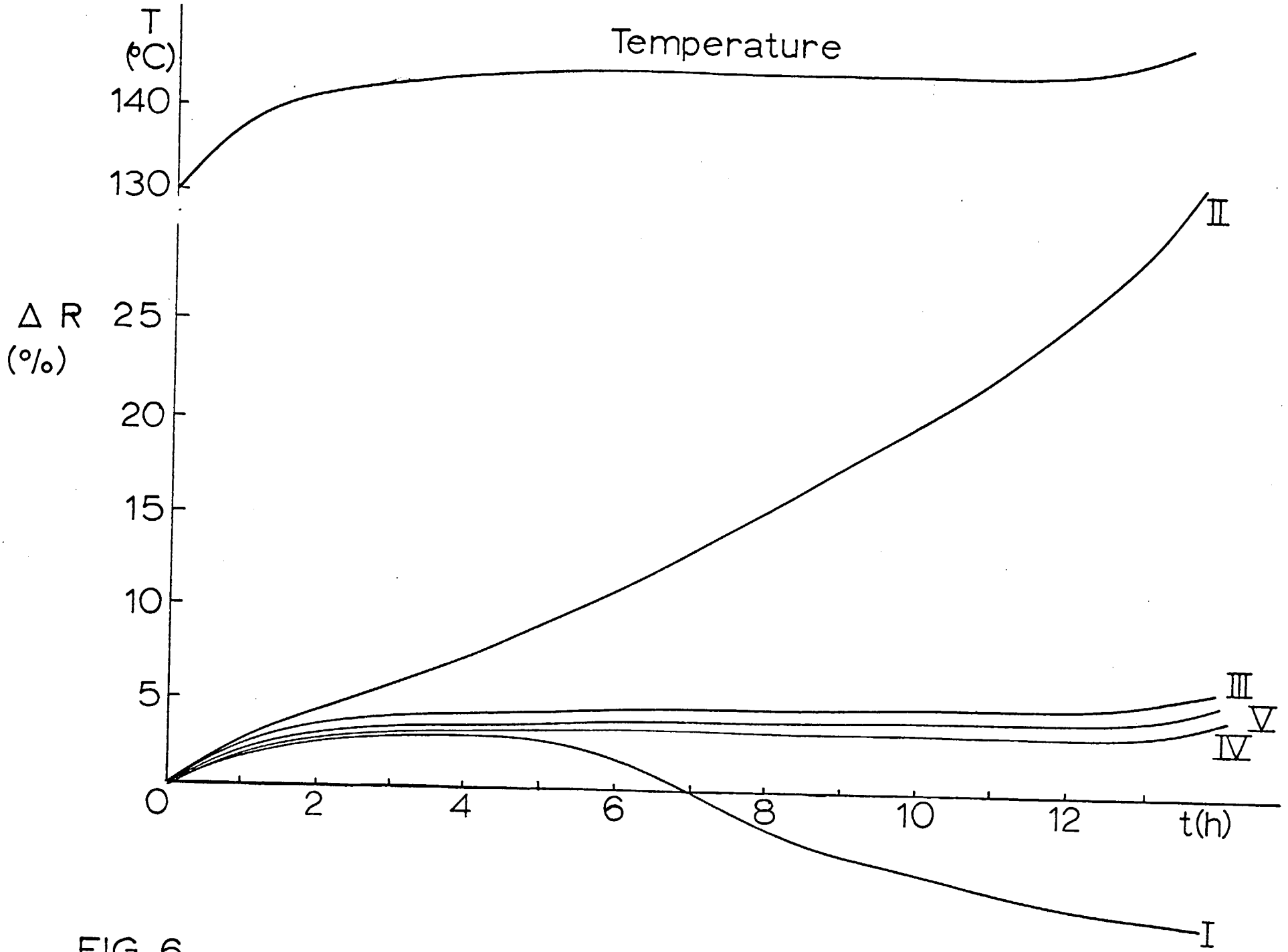
T
(°C)
140
130
Temperature
Δ R
(%)
25
20
15
10
5
0
2
4
6
8
10
12
t(h)
II
III
V
IV
I

FIG. 6

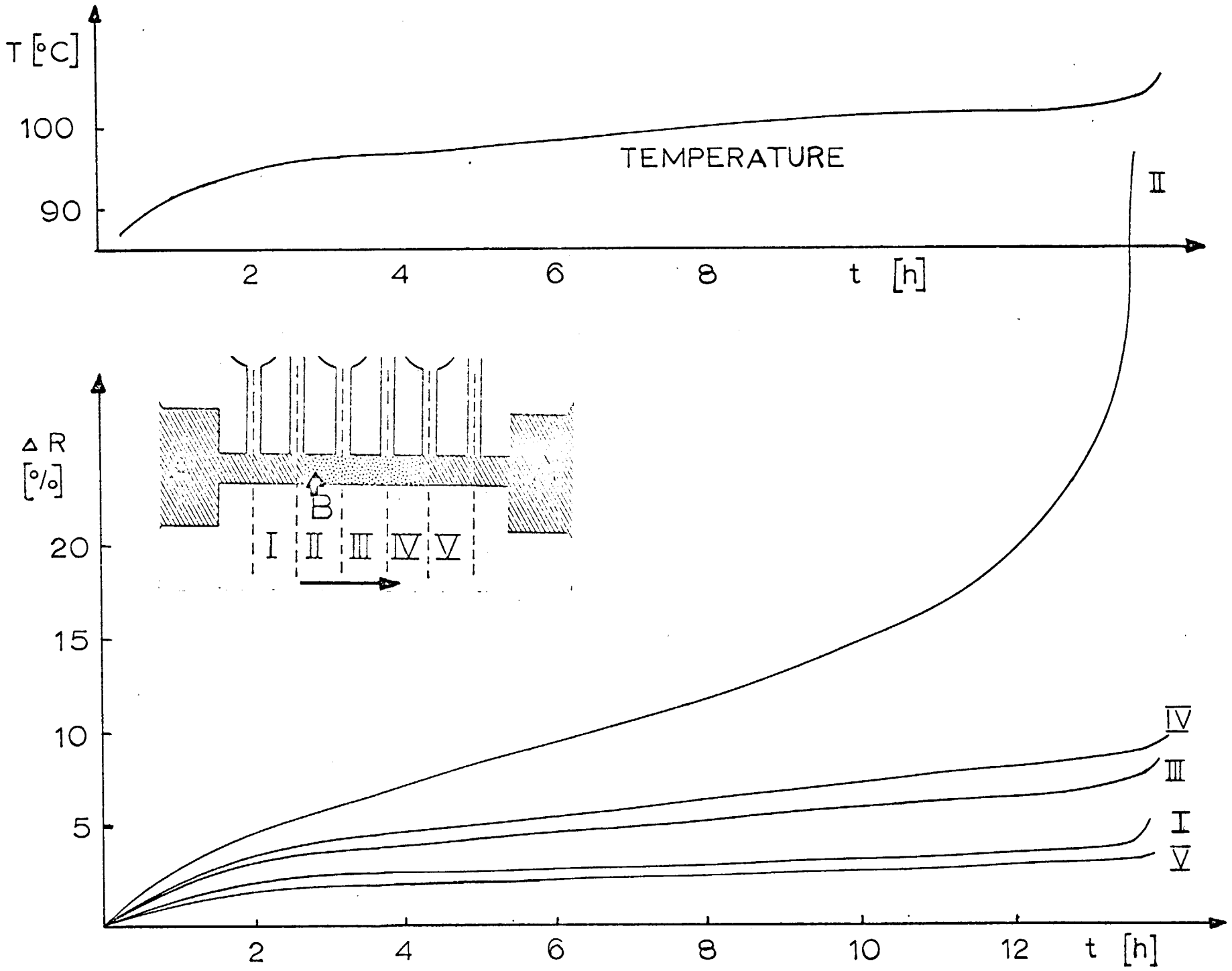
T [°C]
100
90
TEMPERATURE
II
2
4
6
8
t [h]
Δ R
[%]
B
I
II
III
IV
V
20
15
10
5
IV
III
I
V
2
4
6
8
10
12
t [h]

FIG. 7

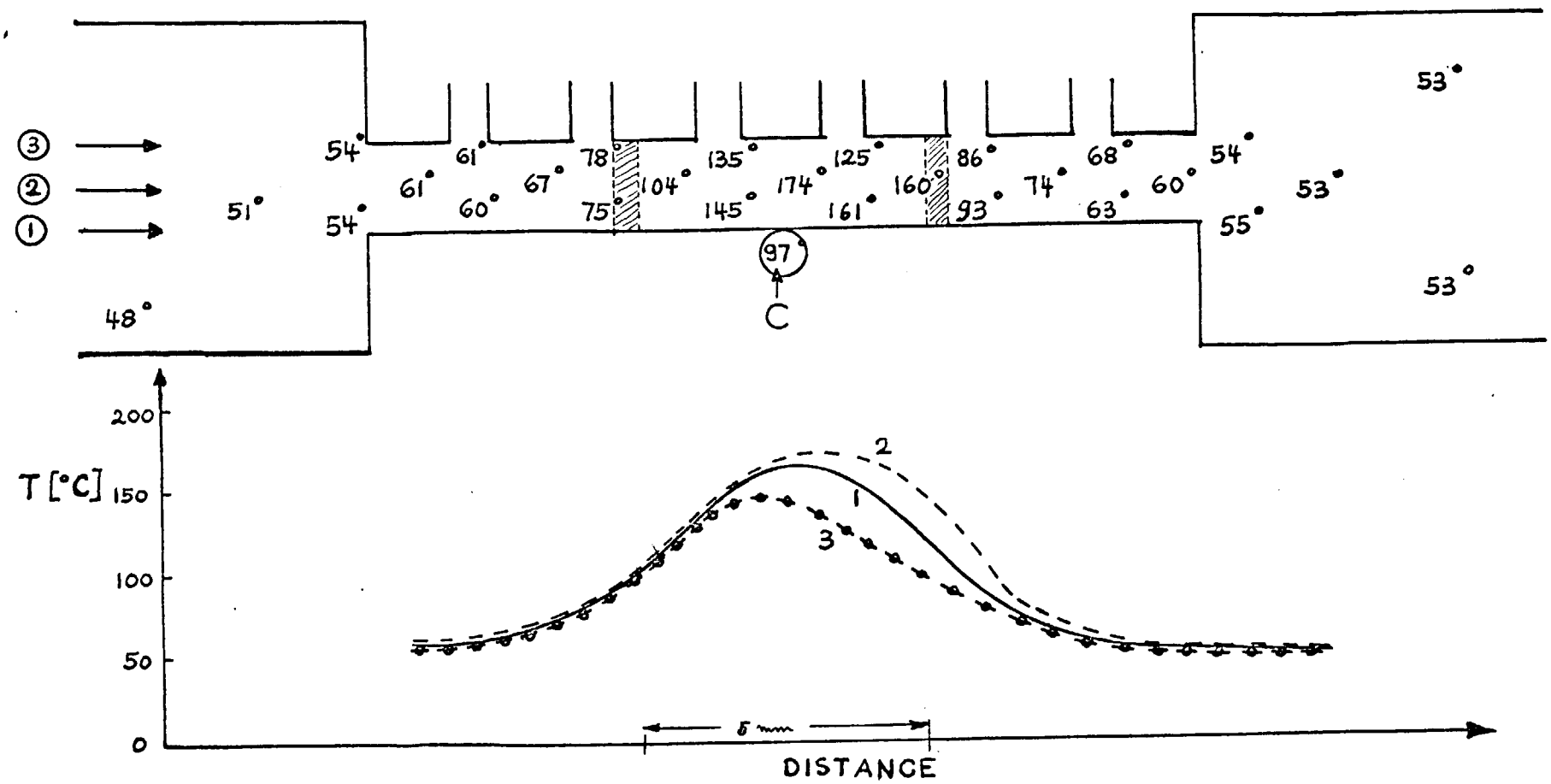
③
②
①
51°
54°
61°
61°
78°
135°
125°
86°
68°
54°
53°
54°
60°
67°
104°
174°
160°
74°
60°
53°
75°
145°
161°
93°
63°
55°
97°
C
48°
53°
200
T [°C]
150
100
50
0
1
2
3
δ mm
DISTANCE

FIG. 8

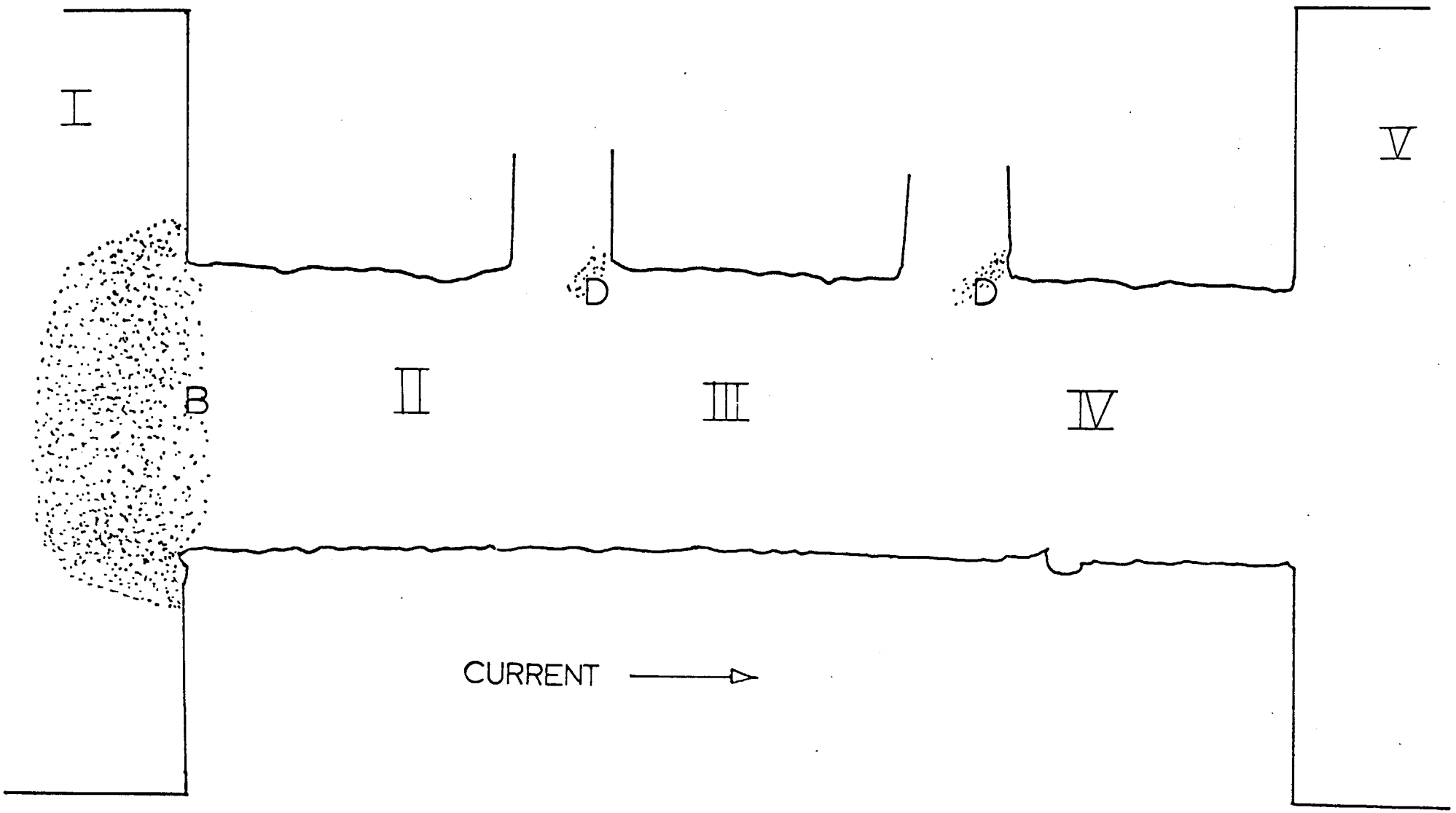


FIG. 9

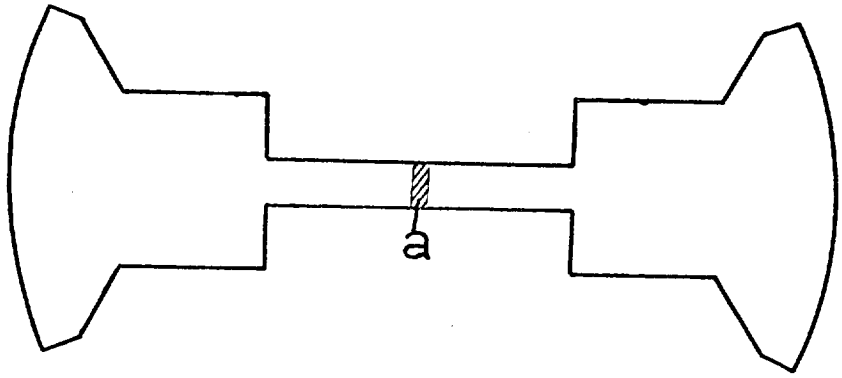


FIG. 10

FIG. 11

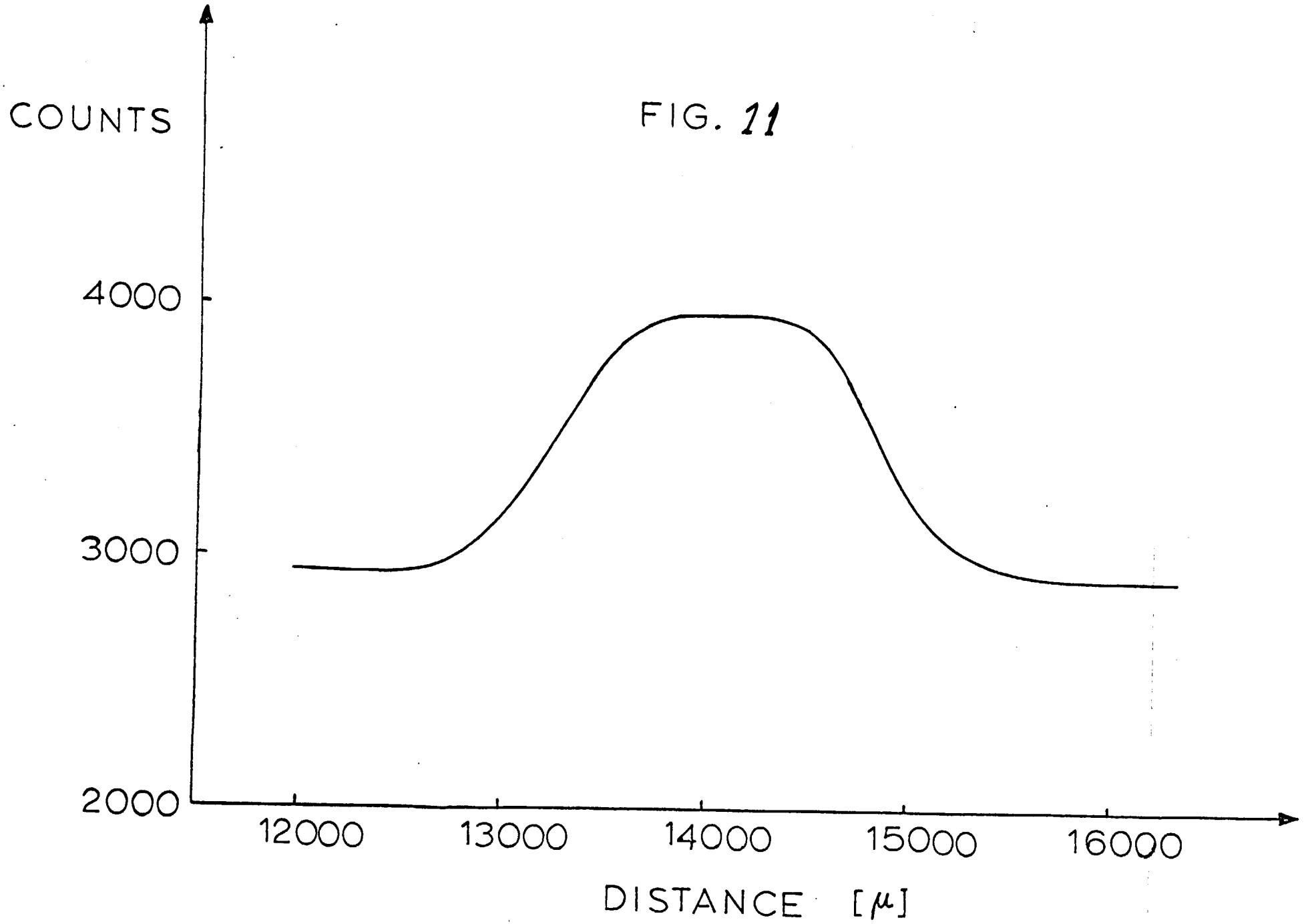
COUNTS
4000
3000
2000
12000
13000
14000
15000
16000
DISTANCE [μ]